Biosketch

Dr Chie Sotozono graduated from the Kyoto Prefectural University of Medicine, Kyoto, Japan in 1986, and subsequently completed her residency training at the Department of Ophthalmology of that same prestigious university. Dr Sotozono received her PhD from the Kyoto Prefectural University of Medicine at 1995. At present, Dr Sotozono is an Assistant Professor in the Department of Ophthalmology at Kyoto Prefectural University of Medicine, and specializes in clinical research and cornea-related diseases and regenerative medicine.

Diffuse disseminated lichenoid-type cutaneous sarcoidosis mimicking erythroderma

Sarcoidosis is a multi-organ granulomatous disease of unknown etiology that can affect the lungs, mediastinal and peripheral lymph nodes, liver, spleen, eyes, parotid gland, and skin.[1] Cutaneous lesions are associated with approximately 20–30% of sarcoidosis cases[2] and can mimic a variety of skin diseases.[1] In our present study, we reported a relatively rare case of diffuse disseminated lichenoid-type cutaneous sarcoidosis mimicking erythroderma.

In 2005, a 70-year-old man presented with the gradual appearance of lightly scaling, large erythematous patches with miliary papules on his trunk and upper arms. The lesions expanded to cover nearly the entire body within 2–3 years from their first appearance and did not respond to very strong class topical steroids (0.05% betamethasone butyrate propionate ointment). The patient denied systemic symptoms, such as fever, arthralgias, or fatigue. However, in 2008 he developed gastric cancer and surgery was performed.

In 2009, he experienced the sudden onset of photophobia in his right eye, followed by diminishing sight in his right eye. Ophthalmological examination of the right eye diagnosed uveitis with granulomatous changes thought to be associated with systemic sarcoidosis. He presented to our dermatology department for evaluation of his skin lesions in 2010.

Physical examination revealed several millimeters in diameter erythematous papules disseminated on the trunk and extremities (Fig. 1a,b). The initial differential diagnoses included erythroderma due to allergic substances or an internal malignancy. However, histologic examination following cutaneous biopsy identified multiple non-caseating epithelioid granulomas surrounded by a mixed

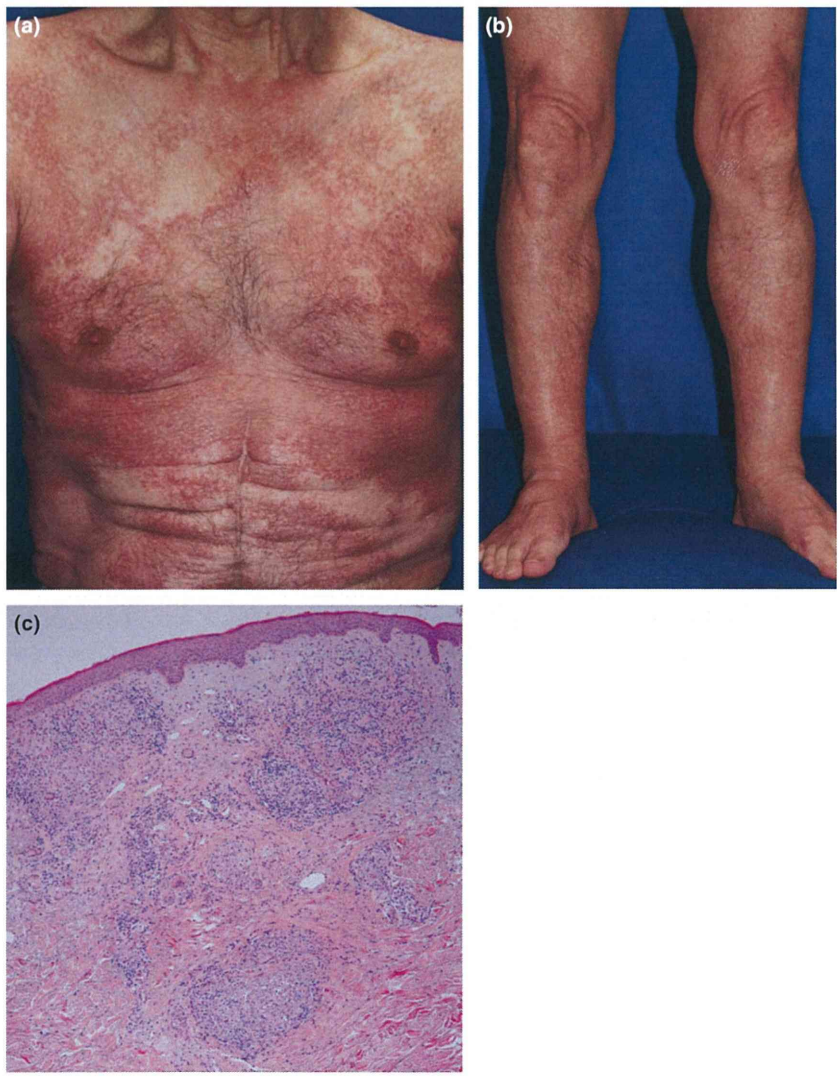

Figure 1 (a,b) Erythematous scaly papules disseminated on the trunk and extremities. (c) Multiple non-caseating epithelioid granulomas surrounded by a mixed infiltrate of lymphocytes in the dermis (hematoxylin and eosin stain, original magnification, ×100)

infiltrate of lymphocytes in the dermis (Fig. 1c). Bilateral hilar lymphadenopathy was evident on the chest radiographs. Laboratory findings, including serum angiotensin-converting enzyme and lysozyme were within normal limits. Tuberculin testing was also negative.

Clinical, laboratory, and histologic findings led to a diagnosis of cutaneous sarcoidosis. Of course, although the erythrodermic-type sarcoidosis was a differential diagnosis, careful examination of skin lesions revealed that the majority consisted of miliary, follicular, erythematous papules, not exfoliative erythema, and the final diagnosis was a diffuse disseminated lichenoid type of cutaneous sarcoidosis. Oral corticosteroids improved the uveitis and lymphadenopathy; however, the cutaneous lesions were resistant to systemic therapy. In addition to the systemic therapy described above, topical steroid and tacrolimus with oral minocycline and tranilast gradually improved (but did not resolve) the skin lesions. Diffuse disseminated types of cutaneous sarcoidosis, which can be classified as erythrodermic, ichthyosiform, or lichenoid, are quite rare.[1,3,4] Our patient presented with internal organ involvement as well. Additionally, his medical history was remarkable for gastric cancer. Internal malignancy can facilitate the formation of granuloma in various organs (i.e., sarcoid reaction),[5] which may have influenced his skin lesions. The precise reason why cutaneous sarcoidosis was disseminated to almost the entire body requires future clarification.

Aya Nishizawa, MD, PhD
Ken Igawa, MD, PhD
Hana Teraki, MD
Hiroo Yokozeki, MD, PhD
Department of Dermatology
Tokyo Medical and Dental University Graduate School of Medicine
Tokyo
Japan

Ken Igawa, MD, PhD.
Yushima 1-5-45
Bunkyo-ku
Tokyo
1138519
Japan
E-mail: k.igawa.derm@tmd.ac.jp

Conflicts of interest: None.

References

1 Haimovic A, Sanchez M, Judson MA, *et al.* Sarcoidosis: a comprehensive review and update for the dermatologist: part I. Cutaneous disease. *J Am Acad Dermatol* 2012; **66**: 699.e691–618.
2 English JC, Patel PJ, Greer KE. Sarcoidosis. *J Am Acad Dermatol* 2001; **44**: 725–743.
3 Greer KE, Harman LE, Kayne AL. Unusual cutaneous manifestations of sarcoidosis. *South Med J* 1977; **70**: 666–668.
4 Yoon CH, Lee CW. Case 6. Erythrodermic form of cutaneous sarcoidosis. *Clin Exp Dermatol* 2003; **28**: 575–576.
5 Cohen PR, Kurzrock R. Sarcoidosis and malignancy. *Clin Dermatol* 2007; **25**: 326–333.

A case of seborrheic keratosis with clear cell change

Seborrheic keratoses are among the most common neoplasms seen in daily practice in dermatopathology. In 2006, Neuhaus *et al.*[1] described nine cases of seborrheic keratosis with linear basal clear cells mimicking melanoma *in situ* in conventional sections, and in 2013, Haspeslagh *et al.*[2] reported the additional case. Recently, we identified a similar but more atypical case on the temporal area of a 55-year-old woman (Fig. 1). Histopathologically, the lesion exhibited the typical architectural pattern of a seborrheic keratosis of the acanthotic type, with acanthosis, papillomatosis, hyperkeratosis, and horn cysts (Fig. 2a). However, in the epidermis, keratinocytes in the whole spinous layer exhibited clear cell change (Fig. 2b), and this point was vastly different from previous reports describing clear cell change only in the basal layer. The monomorphous cells showed a small uniform nucleus and had abundant clear cytoplasm. No nests were seen. This peculiar finding raised the possibility of a

Figure 1 A keratosis with verrucous morphology on left temporal area

STEM CELLS TRANSLATIONAL MEDICINE

EMBRYONIC STEM CELLS/INDUCED PLURIPOTENT STEM (iPS) CELLS

Removal of Reprogramming Transgenes Improves the Tissue Reconstitution Potential of Keratinocytes Generated From Human Induced Pluripotent Stem Cells

KEN IGAWA,[a,b] CHIKARA KOKUBU,[c] KOSUKE YUSA,[d] KYOJI HORIE,[c] YASUHIDE YOSHIMURA,[c] KAORI YAMAUCHI,[e] HIROFUMI SUEMORI,[e] HIROO YOKOZEKI,[b] MASASHI TOYODA,[f] NOBUTAKA KIYOKAWA,[f] HAJIME OKITA,[f] YOSHITAKA MIYAGAWA,[f] HIDENORI AKUTSU,[f] AKIHIRO UMEZAWA,[f] ICHIRO KATAYAMA,[a] JUNJI TAKEDA[c]

[a]Department of Dermatology and [c]Department of Social and Environmental Medicine, Graduate School of Medicine, Osaka University, Osaka, Japan; [b]Department of Dermatology, Graduate School of Medicine, Tokyo Medical and Dental University, Tokyo, Japan; [d]Wellcome Trust Sanger Institute, Wellcome Trust Genome Campus, Hinxton, Cambridge, United Kingdom; [e]Department of Embryonic Stem Cell Research, Institute for Frontier Medical Sciences, Kyoto University, Kyoto, Japan; [f]Department of Reproductive Biology, Center for Regenerative Medicine, National Center for Child Health and Development, Tokyo, Japan

Correspondence: Ken Igawa, M.D., Ph.D., Department of Dermatology, Graduate School of Medicine, Tokyo Medical and Dental University, 1-5-45 Yushima, Bunkyo-ku, Tokyo 113-8519, Japan. Telephone: 81-3-5803-5286; E-Mail: k.igawa.derm@tmd.ac.jp; or Junji Takeda, M.D., Ph.D., Department of Social and Environmental Medicine, Graduate School of Medicine, Osaka University, 2-2 Yamadaoka, Suita-city, Osaka 565-0871, Japan. Telephone: 81-6-6879-3262; E-Mail: takeda@mr-envi.med.osaka-u.ac.jp

Received October 2, 2013; accepted for publication May 21, 2014; first published online in SCTM EXPRESS July 14, 2014.

1066-5099/2014/$20.00/0

http://dx.doi.org/10.5966/sctm.2013-0179

Key Words. Human • Induced pluripotent stem cell • Keratinocyte • Differentiation • Transgene

ABSTRACT

Human induced pluripotent stem cell (hiPSC) lines have a great potential for therapeutics because customized cells and organs can be induced from such cells. Assessment of the residual reprogramming factors after the generation of hiPSC lines is required, but an ideal system has been lacking. Here, we generated hiPSC lines from normal human dermal fibroblasts with *piggyBac* transposon bearing reprogramming transgenes followed by removal of the transposon by the transposase. Under this condition, we compared the phenotypes of transgene-residual and -free hiPSCs of the same genetic background. The transgene-residual hiPSCs, in which the transcription levels of the reprogramming transgenes were eventually suppressed, were quite similar to the transgene-free hiPSCs in a pluripotent state. However, after differentiation into keratinocytes, clear differences were observed. Morphological, functional, and molecular analyses including single-cell gene expression profiling revealed that keratinocytes from transgene-free hiPSC lines were more similar to normal human keratinocytes than those from transgene-residual hiPSC lines, which may be partly explained by reactivation of residual transgenes upon induction of keratinocyte differentiation. These results suggest that transgene-free hiPSC lines should be chosen for therapeutic purposes. STEM CELLS TRANSLATIONAL MEDICINE *2014;3:992–1001*

INTRODUCTION

Reprogramming of differentiated somatic cells into a pluripotent state has been previously carried out by cell fusion or nuclear transfer [1]. The molecular basis of reprogramming has been revealed by exogenous expression of combinations of transcription factors. Recently, four factors, namely *OCT4*, *SOX2*, *KLF4*, and c*MYC*, which are highly expressed in embryonic stem cells (ESCs), have been shown to reprogram both mouse and human somatic cells into ESC-like pluripotent cells, named induced pluripotent stem cells (iPSCs) [2, 3].

ESCs have an unlimited proliferative capacity and extensive differentiation capability and are thought to be a powerful cell source for regenerative medicine [4]. However, there are both ethical and biological concerns for the clinical use of ESCs that are related to their derivation from embryos and potential for immunological rejection, respectively. In addition, it is difficult to generate patient- or disease-specific ESCs that are required for their effective application. These disadvantages can be at least partially avoided by the alternative use of iPSCs.

Induction of reprogramming by defined factors has been mostly carried out by coinfection with retroviral vectors [2, 3]. The major problems of this retrovirus-based method are its oncogenicity and mutagenesis. Reactivation of the proviral *Myc* oncogene is one of the reasons for the oncogenicity of iPSCs [5]. However, although three-factor (*Oct4*, *Sox2*, and *Klf4*) iPSC-derived mice do not develop tumors [6], ectopic expression of any one of these genes may have deleterious consequences. For example, ectopic expression of Oct4 in the skin or intestine causes tumor development [7]. Overexpression of Klf4 induces dysplasia of the skin [8]. Furthermore, retroviral integration itself causes insertional mutagenesis and may alter the expression pattern of nearby genes [9]. Therefore, transgene integration-free iPSCs are necessary for their clinical use.

To achieve such iPSCs, we used the *piggyBac* transposon system to deliver the reprogramming

factors. The *piggyBac* transposon is a moth-derived DNA transposon [10] that is highly active in mammalian cells and that has been used for gene delivery and mutagenesis [11]. The advantage over viral integration is that transposons can be easily removed from the host genome. Among the various DNA transposons, the *piggyBac* transposon does not leave "footprint" mutations upon excision [12]. The TTAA integration sites used by *piggyBac* transposons are repaired to the original sequence upon excision [12], resulting in removal of transposons from the host genome without changing any nucleotide sequences. Using this *piggyBac* transposon system, transgene integration-free and mutation-free mouse iPSCs have already been generated and reported by some groups, including our own [13–15].

In this study, by exploiting this unique property of the *piggyBac* transposon system, we generated transgene-free (Tg−) human induced pluripotent stem cell (hiPSCs) from transgene-retaining (Tg+) parental hiPSCs, thereby preserving the common isogenic genetic background. We generated epidermal keratinocytes from both Tg− and Tg+ hiPSCs in vitro and directly compared their tissue reconstitution potentials, allowing precise evaluation of the net effect of residual transgenes in hiPSCs and their derivatives.

Materials and Methods

Plasmid Construction

Five human reprogramming factors (*POU5F1*, *SOX2*, *KLF4*, *cMYC*, and *LIN28*) were amplified by polymerase chain reaction (PCR) with fusion of the first and second half of the T2A sequence in the C and N termini, respectively, except for the N terminus of *POU5F1* and the C terminus of *LIN28*. PCR products were cloned into pCR4 using a Zero Blunt Topo PCR cloning kit (Life Technologies, Rockville, MD, http://www.lifetech.com), resulting in pCR-O, pCR-S, pCR-K, pCR-M, and pCR-L, respectively. The sequences of the inserts were verified by capillary sequencing. To combine all five factors into a single coding sequence, the BglII-SalI fragment containing the SOX2-coding sequence in pCR-S was first cloned into the BamHI-SalI site of pCR-O, resulting in pCR-OS. KLF4, MYC, and LIN28 fragments were sequentially inserted in the same manner, resulting in the final construct, pCR-OSKML (h5F). The EcoRI-SalI fragment of h5F was cloned into the EcoRI-SalI site of pBluescript, resulting in pBS-h5F. The BamHI-SalI fragment of pBS-h5F was cloned into the BglII-XhoI site of the *piggyBac* transposon vector, pPB-CAG.EBNXN, resulting in PB-CAG-h5F. Finally, the negative selection marker PGK-puΔtk cassette was excised from pFlexible [16] by XhoI digestion and then inserted into the SalI site of pPB-CAG-h5F, resulting in pPB-CAG-h5F-puroTK. Primers for construction of the vectors are listed in supplemental online Table 1.

Cell Culture

Mouse embryonic fibroblasts (MEFs) were cultured in Dulbecco's modified Eagle's medium (DMEM) containing 10% fetal bovine serum (Life Technologies), 2 mM L-glutamine, 1× nonessential amino acids (Life Technologies), and 0.1 mM 2-mercaptoethanol. Normal human dermal fibroblasts (NHDFs) (Lonza, Walkersville, MD, http://www.lonza.com) from neonatal male skin were cultured in the same medium. Normal human epidermal keratinocytes (Lonza), also from neonatal male skin, and keratinocytes derived from iPSCs (iKCs) were cultured in serum-free keratinocyte-specific medium (CnT57; CELLnTEC, Bern, Switzerland, http://cellntec.com). Human iPSC lines and ESC lines (KhES-1 and KhES-3; Kyoto University, Kyoto, Japan, http://www.kyoto-u.ac.jp/en [17]) were cultured on mitomycin C-treated MEFs in serum-free human ESC (hESC) medium consisting of DMEM/F-12 (Life Technologies) with 20% knockout serum replacement (Life Technologies), 2 mM L-glutamine, 1× nonessential amino acids (Life Technologies), 0.1 mM 2-mercaptoethanol, and 5 ng/ml basic fibroblast growth factor (bFGF) (Katayama Chemical Industries Co., Ltd., Osaka, Japan, http://www.katayamakagaku.co.jp).

Generation of hiPSCs

Generation of hiPSCs was conducted according to the protocol described in Figure 1. NHDFs were plated in six-well plates and grown to 60%–70% confluence. On day 0, 2.5 μg of pCMV-mPBase and plasmids containing the *piggyBac* transposon carrying the reprogramming factors (pPB-CAG-h5F-puroTK) were simultaneously transfected into cells using Lipofectamine 2000 (Life Technologies) according to the manufacturer's protocol. On day 5, transfected NHDFs were trypsinized and replated onto feeder cells (1×10^5 MEFs per 60-mm dish) in serum-free hESC medium. The medium was refreshed every other day. On days 10–14, ESC-like colonies appeared in the dishes, and at approximately day 21, colonies were counted, picked, and expanded further.

Preparation of Splinkerettes

Splinkerettes were prepared by annealing Spl-top and Spl-blunt (to generate blunt ends). The sequences of these oligonucleotides are listed in supplemental online Table 1. After heat denaturation at 95°C for 10 minutes, annealing was performed by cooling down the mixture of 11 pmol of each strand in 10 mM Tris-HCl (pH 7.4) and 5 mM $MgCl_2$ in a total volume of 100 μl.

Determination of Transposon Integration Sites

Transposon integration sites were determined by splinkerette PCR. Genomic DNA from primary iPSCs was digested by appropriate restriction enzymes (HaeIII and RsaI) for 2 hour in 20-μl reactions. After heat inactivation, 2 μl of the digestion mixture was ligated with the 0.5 μl of splinkerette adaptors in 20-μl reactions. One microliter of the ligation mixture was then subjected to nested PCR. A primer pair, Spl-P1 and PB5-P1, was used for the first PCR. In the second PCR, the Spl-P2 and PB5-P2 primer pair was used (primer sequences are listed in supplemental online Table 1). Finally, PCR products were directly sequenced to determine the genomic sequences flanking the *piggyBac* terminal repeats. Sequences were analyzed by Blat searching the UCSC Genome Browser.

Bisulfite Sequencing Analysis

Bisulfite conversion of DNA was performed using a MethylEasy Xceed Rapid DNA Bisulphite Modification Kit (Genetic Signatures, Randwick, Australia, http://geneticsignatures.com) according to the manufacturer's protocol, and then sequencing was performed. Primers for amplification of bisulfited DNA are listed in supplemental online Table 1.

Southern Blot Analysis

To detect the copy number of integrated transposons, genomic DNA from each hiPSC line was digested and hybridized with

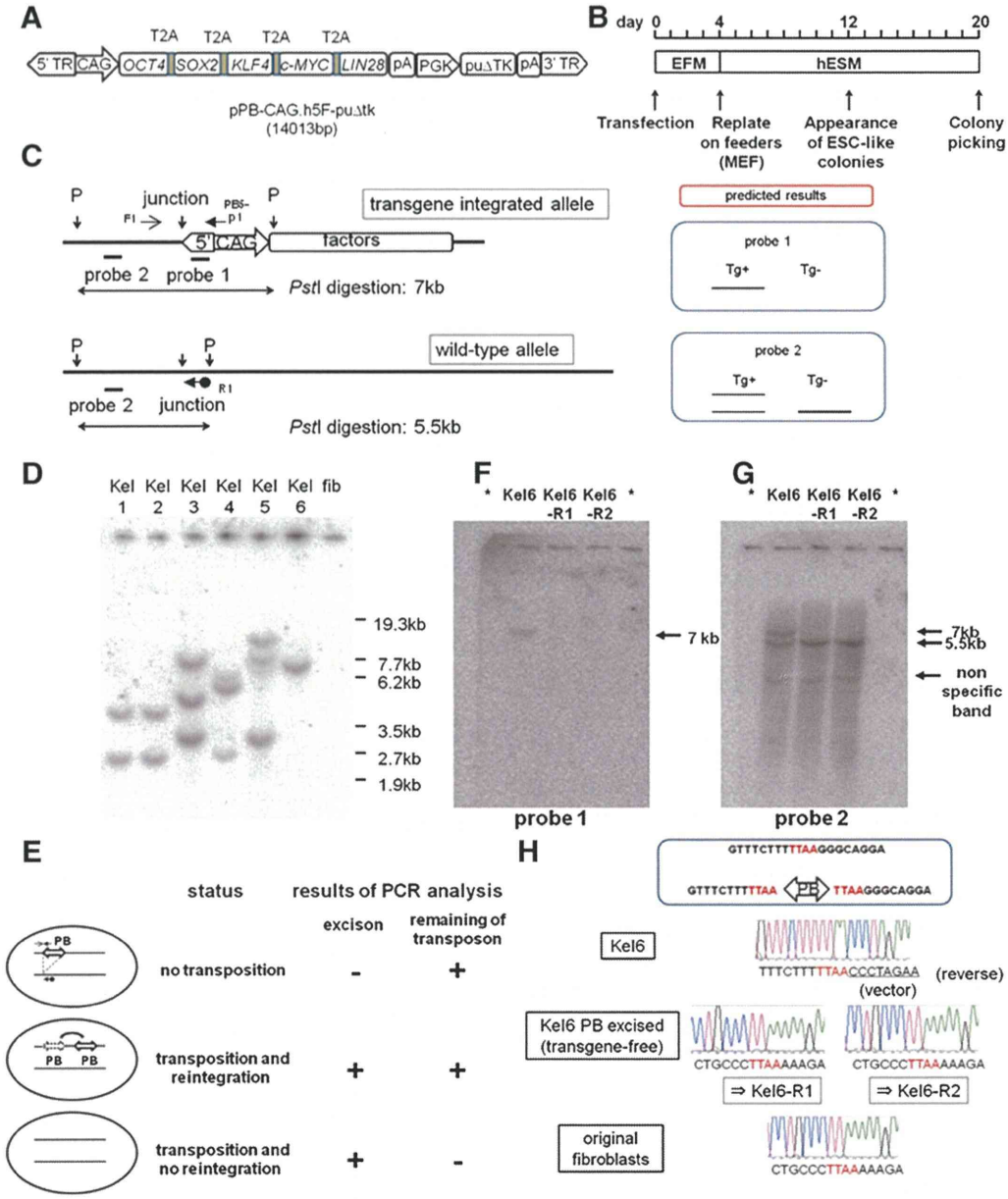

Figure 1. Generation of human induced pluripotent stem cells (hiPSCs) using the *piggyBac* transposon system and establishment of transgene-free hiPSCs. **(A):** Schematic representation of the *piggyBac* transposon vector carrying reprogramming factors (pPB-CAG.h5F-puΔtk, 14,013 bp). Genes encoding five factors were linked by sequences encoding 2A peptides. Expression of these factors was driven by constitutively active CAG promoters. **(B):** Timeline of reprogramming. **(C):** Representative restriction enzyme map and positions of primers used to evaluate transposon removal in the hiPSC genome at the site of transposon vector integration. Probes 1 and 2 were designed as indicated by the thick line. A schematic representation of the predicted results of Southern blot analysis using probe 1/2 is shown (right). The thick line indicates a higher density band. F1, R1, and PB5-p1 are primers used to evaluate transposon removal. Primer sequences are listed in supplemental online Table 1. **(D):** Southern blot analysis of primary hiPSCs. Genomic DNA was digested with PstI and hybridized with probe 1. Lanes 1–6, primary hiPSCs generated by transposon-mediated reprogramming. Lane 7, original fibroblast genomic DNA as a negative control. **(E):** Schematic representation of the strategy of transposon removal. Each arrow indicates a designated primer used for a two-step PCR screening (Fig. 1C; supplemental online Fig. 2). Representative PCR results for each status are shown in supplemental online Fig. 3. **(F, G):** The results of Southern blot analysis indicating transposon-free hiPSCs were confirmed by PCR screening. **(F)** and **(G)** show the results using probes 1 and 2, respectively. Lanes marked by asterisks contained sample loading buffer only (without DNA). **(H):** Sequencing analysis of the integration site on chromosome 7 in Kel6 and transposon-excised Kel6 (Kel6-R1 and Kel6-R2). The reference sequences (top) indicate the transposon integration sites where TTAA sequences were duplicated at both ends of the transposon. The electrophoretograms demonstrate that the sequences in Kel6-R1 and Kel6-R2 are identical to the original sequences in the fibroblasts and reference sequences. Abbreviations: EFM, embryonic fibroblast medium; ESC, embryonic stem cell; fib, fibroblast; hESM, human embryonic stem cell medium; junction, junction site of the genome and transposon vector; MEF, mouse embryonic fibroblast; p, PstI; PB, *piggyBac* transposon vector; PCR, polymerase chain reaction; puΔtk, puΔtk expression cassette; Tg+, transgene-residual; Tg−, transgene-free; 3′TR, 3′ terminal repeat of the *piggyBac* transposon; 5′TR, 5′ terminal repeat of the *piggyBac* transposon.

partial sequences of the *piggyBac* transposon 5′ terminal repeat as the probe. Primer sequences for generating the probe are listed in supplemental online Table 1.

Transposon Removal From Primary hiPSCs

Fifteen micrograms of the *piggyBac* transposase expression vector with the blasticidin (bsd) selection cassette was electroporated into 1×10^6 dissociated hiPSCs. A total of 2×10^5 cells were seeded onto 6-cm dishes containing feeder cells (MEFs) in hESC medium containing 10 μM ROCK inhibitor. From the following day, 2 μg/ml bsd was added to the culture medium, and selection was continued for 3 days. After an additional 7 days of culture without bsd, the resulting colonies were dissociated to single cells and expanded in hESC medium containing 10 μM ROCK inhibitor. Transposon removal was screened by two-step PCR analysis with the primers listed in supplemental online Table 1. The results of the PCR screening were confirmed by Southern blot analysis using the 5′ terminal repeat of the *piggyBac* transposon as one of the probes and genomic sequences just outside of the transposon integration site as the other probe. Primer sequences for generating the probe are listed in supplemental online Table 1.

Keratinocyte Induction From hiPSCs

We used the differentiation protocol described in Results to obtain keratinocytes from hiPSCs and hESCs. One week of random differentiation was induced in differentiation medium (hESC medium without bFGF). Then the culture medium was changed to serum-free keratinocyte-specific medium, and the cells were cultured for an additional 4–5 weeks.

Immunostaining

Cells were fixed in 3% formaldehyde in phosphate-buffered saline (PBS) for 15 minutes at room temperature and then permeabilized in 100% methanol for 10 minutes at −20°C when needed. Then the cells were blocked in serum-free protein block (Dako, Glostrup, Denmark, http://www.dako.com) for 1 hour at room temperature. The cells were incubated with antibodies against NANOG (Cell Signaling Technology, Beverly, MA, http://www.cellsignal.com; 1:200, rabbit polyclonal), OCT4 (Cell Signaling Technology; 1:200, rabbit polyclonal), SOX2 (Cell Signaling Technology, 1:200, rabbit polyclonal), SSEA4 (Cell Signaling Technology; 1:200, mouse IgG3 monoclonal), TRA-1-60 (Cell Signaling Technology; 1:200, mouse IgM monoclonal), TRA-1-81 (Cell Signaling Technology; 1:200, mouse IgM monoclonal), human keratin 5/14 (Covance, Princeton, NJ, http://www.covance.com; 1:500, rabbit IgG polyclonal), and each negative control antibody (Dako) overnight at 4°C. After washing with PBS (three times for 5 minutes), cells were labeled with Alexa Fluor 488- or Alexa Fluor 555-conjugated secondary antibodies (Life Technologies) for 1 hour at room temperature. After washing with PBS (three times for 5 minutes), specimens were analyzed under a fluorescence microscope (BZ-9000 BIOREVO; Keyence, Osaka, Japan, http://www.keyence.com).

Deparaffinized and rehydrated tissue sections were immersed in preheated (~100°C) target retrieval solution (Dako) for 10 minutes. After cooling at room temperature, the sections were washed three times with PBS, and nonspecific binding sites were blocked by incubation with serum-free protein block for 1 hour at room temperature. Then the sections were incubated with antibodies against human keratin 14 or involucrin (GeneTex, San Antonio, TX, http://www.genetex.com; 1:500, rabbit IgG polyclonal) at 4°C overnight. After three washes with PBS, tissue sections were reacted with an Alexa Fluor 555-conjugated secondary antibody for 1 hour at room temperature. After further washing, the sections were mounted with Fluoprep (bioMérieux, Marcy l'Etoile, France, http://www.biomerieux.com).

Real-Time PCR

Total RNA was extracted using an SV Total RNA Isolation System (Promega, Madison, WI, http://www.promega.com). One microgram of total RNA was reverse transcribed using random primers by Moloney murine leukemia virus reverse transcriptase (Life Technologies) and then subjected to PCR using the primers listed in supplemental online Table 1. Quantitative RT-PCR was performed using Power SYBR Green PCR Master Mix (Life Technologies) and an ABI7900HT sequence detector (Life Technologies) according to the manufacturer's protocols. Quantification of gene expression was based on the ΔCt method and normalized to β-actin expression. Melting curve and electrophoresis analyses were undertaken to verify the specificities of the PCR products and to exclude nonspecific amplification.

Single-Cell Gene Expression Analysis (Fluidigm Dynamic Array)

Single-cell gene expression profiling was performed using a Biomark dynamic array (Fluidigm, South San Francisco, CA, http://www.fluidigm.com) according to the manufacturer's protocol. Briefly, the cells were single-cell sorted using a BD FACSAria (BD Biosciences, San Diego, CA, http://www.bdbiosciences.com) into 2× CellsDirect buffer (Life Technologies). Cells were subjected to target-specific reverse transcription and 18 cycles of PCR preamplification with a mix of primers specific to the target genes (STA). STA products were then processed for real-time PCR analysis on Biomark 48:48 dynamic array integrated fluidic circuits (Fluidigm). The results obtained from the analysis were conducted with the R statistics package and output as a heat map. The primers for the analysis are listed in supplemental online Table 2.

Results

Successful Establishment of hiPSCs Using the *piggyBac* Transposon System

To deliver the reprogramming factors to recipient cells, we constructed *piggyBac* transposon-based reprogramming vectors as described in Materials and Methods (Fig. 1A). cDNAs constituting the open reading frames of *OCT4*, *SOX2*, *KLF4*, *cMYC*, and *LIN28* were combined into a single open reading frame separated by sequences encoding 2A peptides and placed under the constitutively active CAG promoter. The ~20-amino acid 2A peptides from the *Thosea asigna* virus (T2A) work as self-cleaving signals and enable the expression of several gene products from a single transcript [18], thereby facilitating multigene delivery to target cells.

NHDFs were transfected with the above-mentioned *piggyBac* transposon vector carrying the five factors to induce reprogramming. The protocol we used is illustrated in Figure 1B. We performed cationic lipofection to introduce 2.5 μg of *piggyBac*

transposon and 2.5 μg of *piggyBac* transposase expression vector into ~70% confluent NHDFs cultured in six-well plates and maintained the cells in embryonic fibroblast medium for 4 days. At day 5, the transfected NHDFs were replated onto feeder cells (mitomycin C-treated MEFs) and maintained in human ESC (hESC) medium. At approximately day 14, small ESC-like colonies appeared. At day 20, colonies were picked up and passaged. In summary, we transfected 1×10^5 NHDFs with a transfection efficiency of approximately 10%, which was confirmed with the preliminary results using green fluorescent protein as reporter, and obtained approximately 100 colonies. Therefore, the overall reprogramming efficiency was approximately 1%, which is virtually equivalent to that of the retroviral method.

Derivation of Transgene Integration-Free and Mutation-Free hiPSCs by *piggyBac* Transposon Vector Removal

We investigated the copy number of the integrated transposons by Southern blot analysis with a probe designed in the 5′ repeat of the *piggyBac* transposon (probe 1 in Fig. 1C). As shown in Figure 1D, most hiPSCs colonies had multiple insertions. Among the colonies, we obtained a colony with single-copy integration (named KeI6). In the following experiments, our established hiPSC clone, KeI6, or its derivatives were mainly used.

To obtain transgene-free hiPSCs, we first used splinkerette PCR to identify the integration sites and found that the transposon was integrated at chromosome 7 (supplemental online Fig. 1). Next, we attempted to eliminate transposons from the hiPSC genome. As described in Materials and Methods, we used a two-step PCR screening system to select transposon-free iPSCs after transfection of the *piggyBac* transposase expression plasmid (Fig. 1E). The first PCR was conducted with a primer pair that detected excision of the transposon from the original site (Fig. 1C). The second PCR was conducted with a primer pair that detected the transposon itself (supplemental online Fig. 2). Representative results of this PCR screening are shown in supplemental online Figure 3.

After transient transposase expression and bsd selection, because transposase expression vector possesses bsd selection cassette, we picked colonies and screened them by PCR as described above. We obtained 10 clones of 55 colonies from the transposase-transfected KeI6 line, in which excision of the transposon had occurred (positive in the first step PCR analysis). After the second PCR analysis, we obtained two transposon-free candidate clones of the 10 clones. We then expanded two transposon-free clones (named KeI6-R1 and KeI6-R2) and confirmed them by Southern blot analysis using the 5′ repeat of the *piggyBac* transposon as the probe (probe 1 in Fig. 1C). We confirmed the loss of transposons in both clones that we identified as transposon-free by PCR (Fig. 1F). We also performed further Southern blot analysis using a probe designed just outside of the transposon-genome junction (probe 2 in Fig. 1C), which confirmed the results described above (Fig. 1G). Thus, we concluded that the transposons had been successfully removed in KeI6-R1 and KeI6-R2.

The *piggyBac* transposon does not leave a footprint at the excised site. To confirm that the transgene-free hiPSCs had no footprint mutations, we amplified the genomic regions encompassing the integration excision sites by PCR and then sequenced the PCR products directly. If there was a footprint mutation (e.g., a nucleotide change, insertion, or deletion), the sequence after TTAA, the target site of *piggyBac* integration, would be a mixture of sequences from the wild-type and excised alleles. The signals from all integration sites were identical to those from the original genomic sequence (Fig. 1H), indicating the absence of footprint mutations. Thus, we "cured" transgene-harboring hiPSCs by removing the transposon.

Characteristics of the Established hiPSCs

Next, we investigated the characteristics of the established hiPSCs. Immunofluorescence staining showed that both transgene-residual and -free hiPSC lines uniformly expressed stem cell markers such as OCT4, SOX2, NANOG, and SSEA4 (Fig. 2A). We also conducted RT-PCR analysis of *OCT4* and *NANOG* gene expression and found that these genes were expressed in our hiPSCs at approximately the same levels as those in retrovirus-based hiPSCs, whereas gene expression associated with the transposon appeared to be silenced (Fig. 2B; supplemental online Fig. 2). To evaluate the epigenetic reprogramming status, we investigated the DNA methylation status at *OCT4* promoter regions by bisulfite sequencing analysis and found that these promoter regions were almost completely unmethylated in the hiPSCs, which was in contrast to the status of the original fibroblasts (58% of the CpGs were methylated; Fig. 2C). This result indicated that the epigenetic reprogrammed status was maintained in our established hiPSCs even after the transgenes were eliminated. As shown in Figure 2D, karyotypic analysis revealed that both KeI6 and KeI6-R1 had a normal karyotype, 46XY. To confirm the pluripotency of the hiPSCs, we performed in vitro differentiation analysis. Both transgene-residual and -free hiPSC lines successfully differentiated into the three germ layers, namely ectoderm (K14-positive cells), mesoderm (desmin-positive cells), and endoderm (α-fetoprotein-positive cells) (Fig. 2E). These results suggested that the transgene-residual and -free hiPSC lines had phenotypes similar to those of pluripotent cells in terms of gene expression, epigenetic modifications, and the potential for differentiation into the three germ layers.

Keratinocyte Induction From hiPSCs

We next attempted to differentiate the established hiPSCs into epidermal keratinocytes. There are few reports that describe protocols for differentiation of hiPSCs or hESCs into keratinocytes, in which retinoic acid (RA) and/or bone morphogenetic protein 4 (BMP4) are preferably used [19, 20]. In the present study, as described in Materials and Methods, we used a modified protocol in which neither RA nor BMP4 were used; this protocol is briefly illustrated in Figure 3A. At 4–5 weeks after induction of the differentiation, we obtained cells that had a keratinocyte-like morphology. These cells proliferated and were passaged at least five times in serum-free keratinocyte medium without feeder cells. Moreover, these cells were positive for K5/K14 as indicated by immunohistochemistry (Fig. 3D), suggesting successful differentiation of keratinocytes from hiPSCs. We called these cells induced keratinocytes (iKCs).

Comparing our established transgene-residual iKCs with transgene-free iKCs, there were obvious morphological differences in which transgene-residual iKCs showed a somewhat spindle-shaped morphology (Fig. 3B). Subsequent culturing resulted in transgene-residual iKCs showing a more spindle-shaped morphology. Moreover, some morphologically undifferentiated colonies were developing in the culture (Fig. 3C). Therefore, we checked

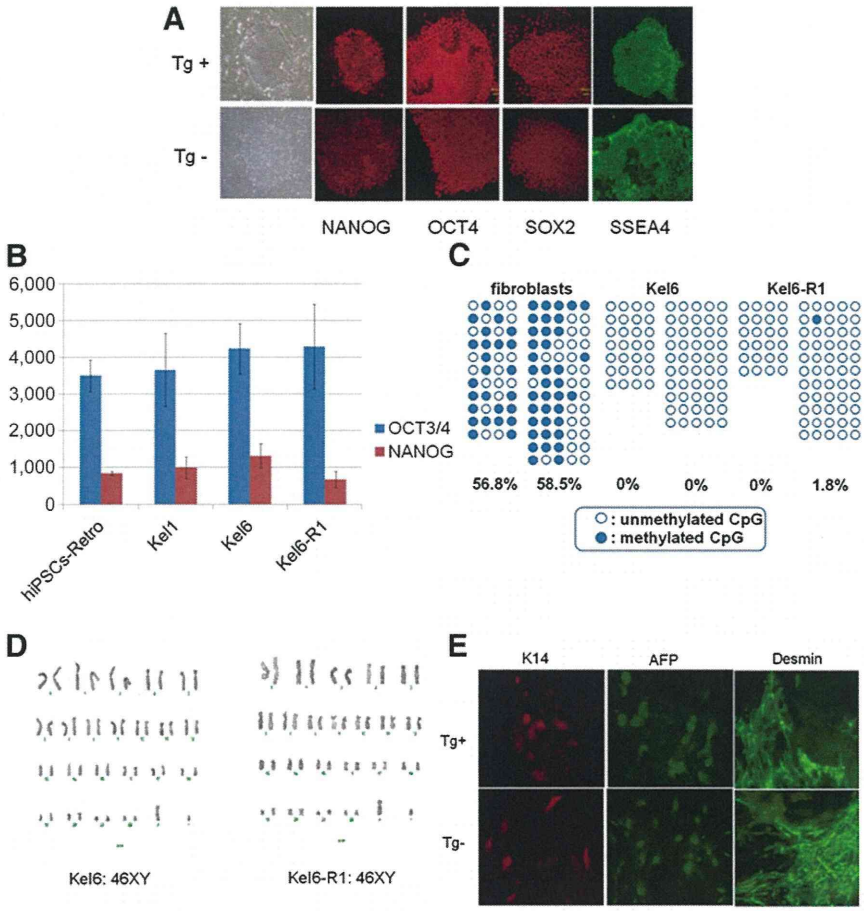

Figure 2. Characteristics of the established hiPSCs. **(A):** Immunofluorescence analysis of NANOG, OCT4, SOX2, and SSEA4 expression in transgene-residual (Kel6) and transgene-free (Kel6-R1) hiPSCs. **(B):** Quantitative RT-PCR analysis of ESC-specific genes (OCT3/4 and NANOG) in transgene-residual (Kel1 and Kel6) and transgene-free (Kel6-R1) hiPSCs. Each bar indicates the means and SEM. **(C):** Bisulfite sequencing of the OCT4 promoter region. Open and closed circles indicate unmethylated and methylated CpG dinucleotides, respectively. **(D):** Normal karyotype of the transgene-residual (Kel6) and transgene-free (Kel6-R1) hiPSCs. **(E):** We confirmed the differentiation capabilities of transgene-residual (Kel6) and transgene-free (Kel6-R1) hiPSCs into all three germ layers by direct differentiation in vitro: K14, ectoderm; AFP, endoderm; and desmin, mesoderm. Abbreviations: AFP, α-fetoprotein; hiPSCs-Retro, retrovirus-mediated reprogrammed human induced pluripotent stem cells (MRC-5); Tg+, transgene-residual; Tg−, transgene-free.

the epigenetic reprogramming status by the expression of stem cell markers, including *OCT4* and *NANOG*, and various differentiation markers in these iKCs by bisulfite sequencing analysis and real-time PCR, respectively. As expected, the DNA methylation status at *OCT4* promoter regions showed hypomethylation in the original hiPSCs (Kel6 and Kel6-R1) and hypermethylation in iKCs (iKC6 and iKC6-R1) (Fig. 3E). However, by comparing transgene-residual iKCs (iKC6) with transgene-free iKCs (iKC6-R1), the levels of DNA methylation were clearly higher in transgene-free iKCs (38% vs. 62%, respectively; Fig. 3E). To clarify the characteristics of iKCs, we performed single-cell gene expression profiling using Fluidigm dynamic arrays [21]. In line with the results of bisulfite sequencing analysis, stem cell markers, including *OCT4*, *SOX2*, *KLF4*, *MYC*, *LIN28*, and *NANOG*, were obviously expressed in transgene-residual iKCs (though at lower levels than those in hiPSCs), indicating that residual transgenes may have been reactivated in iKCs (Fig. 4; supplemental online Figs. 2, 4). Examination of the expression of keratinocyte-specific genes, including K5, K14, and dNp63, revealed higher expression in iKCs derived from transgene-free iPSCs than in those derived from transgene-residual iPSCs (both transposon- and retrovirus-based hiPSCs) (Fig. 4; supplemental online Fig. 5). On the other hand, K8 and K18, which are expressed during the early stage of epidermal cell lineages, were strongly positive in transgene-residual iKCs (Fig. 4). Based on these results, residual transgenes in hiPSCs could influence epidermal differentiation by reactivation, resulting in partial differentiation into K5/K14-positive keratinocytes.

For further examination, retrovirus-based hiPSCs (transgene residual) and hESCs (no transgenes) were differentiated into keratinocytes using the same protocols described in Figure 3A. At 4–5 weeks of differentiation, cells that could be maintained in keratinocyte-specific medium and that were positive for K5/K14 were obtained. Interestingly, iKCs derived from retrovirus-based hiPSCs morphologically resembled those derived from transgene-residual transposon-based hiPSCs, which showed a spindle-shaped morphology (Fig. 3B). The expression levels of stem cell marker genes, including *OCT4* and *NANOG*, in iKCs derived from retrovirus-based hiPSCs were as low as those in normal human somatic tissues (supplemental online Fig. 4). However, gene expression from the residual retrovirus vector was found to be reactivated in iKCs derived from retrovirus-based hiPSCs (supplemental online Fig. 6). Additionally, two other independent

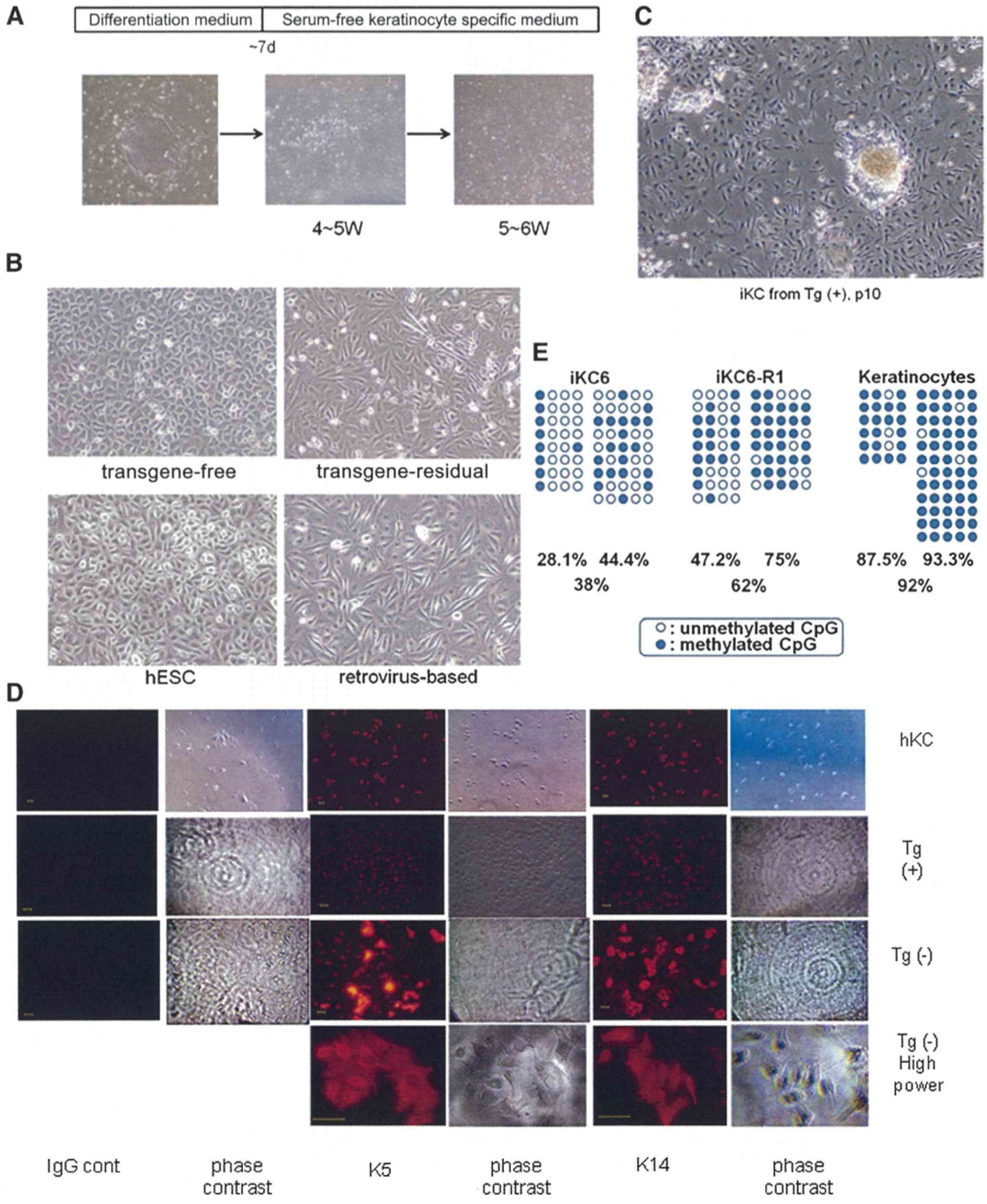

Figure 3. Keratinocytes induced from established hiPSCs. **(A):** Timeline of keratinocyte differentiation. Lower panels show representative photographs of cells at each stage (×40). **(B):** Morphology of cells derived from hiPSCs or hESCs indicated in panels, respectively (×100). **(C):** Morphology of cells derived from transgene-residual hiPSCs at a later passage (p10, ×40). **(D):** Immunofluorescence analysis of K5 and K14 expression in primary keratinocytes (hKCs) and iKCs derived from transgene-residual (KeI6) and transgene-free (KeI6-R1) hiPSCs. Scale bars = 50 μm. **(E):** Bisulfite sequencing of the OCT4 promoter region in iKCs and primary human keratinocytes. Open and closed circles indicate unmethylated and methylated CpG dinucleotides, respectively. Abbreviations: cont, control; d, days; hESC, human embryonic stem cell; hKC, human keratinocyte; IgG cont, IgG control; iKC, induced keratinocyte; Tg(+), transgene-residual; Tg(−), transgene-free; W, weeks.

hiPSC lines, KeI1 and KeI5 (Fig. 1D), both of which retain reprogramming transgenes, were subjected to the keratinocyte differentiation protocol. The KeI1- and KeI5-derived iKCs (iKC1 and iKC5, respectively) showed spindle-shaped morphologies similar to those of transgene-residual iKCs (iKC6) (Fig. 3B; data not shown).

Functional Properties of iKCs

As described above, the morphological and molecular phenotypes of iKCs derived from transgene-free hiPSCs or hESCs appeared to be more similar to those of normal human keratinocytes. Finally, we compared the tissue reconstitution potential of these iKCs using a three-dimensional (3D) culturing system for

